

Glass formation and phase selection of melt-spun Al–Zn–Ce alloys

C. F. Li · C. J. Zhang

Received: 20 May 2009 / Accepted: 15 July 2009 / Published online: 29 July 2009
© Springer Science+Business Media, LLC 2009

Abstract The glass-formation characteristics and phase-selection behavior of Al–Zn–Ce alloys have been studied by X-ray diffraction (XRD) and differential scanning calorimetry (DSC). As the concentration of Ce increases, an intermetallic compound $\text{Al}_2\text{Zn}_2\text{Ce}$ appears, which prevents the occurrence of phase separation, and improves the forming ability of the single amorphous phase. In $\text{Al}_{83}\text{Zn}_{10}\text{Ce}_7$ alloys, the precipitation of fcc-Al was accompanied with the $\text{Al}_2\text{Zn}_2\text{Ce}$ phase and Al_4Ce phase. Moreover, the presence of fcc-Al appears to favor the nucleation and growth of the $\text{Al}_2\text{Zn}_2\text{Ce}$ and Al_4Ce phase. However, it seems that the $\text{Al}_2\text{Zn}_2\text{Ce}$ and Al_4Ce nucleate competitively with the fcc-Al phase and the growth of fcc-Al and $\text{Al}_2\text{Zn}_2\text{Ce}$ prefers to that of Al_4Ce . The competitive nucleation and growth limitation of the various phases are favorable to the formation of Al–Zn–Ce amorphous alloys. For the amorphous Al–Zn–Ce alloys, the glass formation is not controlled by nucleation restrictions but largely by the suppression of growth of nuclei formed during rapid melt quenching.

Introduction

In recent years, Al-based amorphous alloys containing transition metals (TMs) and rare earth elements (Re) have attracted considerable scientific and technological interests due to their good mechanical properties [1–3]. Study on these materials has found that partially crystallized alloys

via the precipitation of α -Al nanocrystals within the amorphous matrix, also termed nanocomposites, may display outstanding strength [4] and promising wear [5] as well as corrosion resistance [6]. However, the mechanism underlying this process is not clearly understood. We have noted that the Al-based metallic glasses have unique glass-forming ability and they do not follow the empirical rules developed for other glass-forming systems [7, 8].

The X-ray diffraction (XRD) patterns of many Al-based amorphous alloys show a prepeak attributed to a strong chemical short-range order [9]. Recent research has shown a strong compound-forming tendency in favor of amorphous-phase formation [10–12]. In general, the more chemical short-range order, the easier it is for the melt to crystallize. And high cooling rates are needed for amorphisation of Al-based alloys. Both during the quench and the annealing intermetallic phase may form. Furthermore, complex phase-selection behavior has been reported in devitrification [13, 14]. In this article, we select the Al–Zn system, a typical decomposition alloy system, as our model system, to study the glass-formation characteristic and the sequence of phases produced in the alloys. It will be essential in understanding glass-formation mechanism, nanocrystallization reaction, and in allowing for bulk glass synthesis of Al-based alloys.

Experiments

Alloy Ingots with nominal composition were prepared from the high-purity elements by high-frequency induction heating. Ribbon samples were obtained by the single-roller melt-spinning technique under a partial argon atmosphere. The diameter of the copper roller is 35 cm and the ribbons were about 2–3 mm in width and $\sim 25 \mu\text{m}$ in thickness.

C. F. Li · C. J. Zhang (✉)
Department of Materials Science and Engineering,
Shandong Institute of Light Industry, Jinan 250353,
People's Republic of China
e-mail: chuanfuli@yahoo.com.cn

The structure of the ribbon samples was examined by XRD with monochromatic Cu K α radiation. Both isothermal and non-isothermal DSC experiments were performed with Netzsch DSC-404 system under a pure argon atmosphere.

Results

Figure 1 shows the XRD patterns of Al₉₀Zn₁₀, Al₉₀Zn₅Ce₅, and Al₈₃Zn₁₀Ce₇ as rapidly solidified alloys. The Al₉₀Zn₅Ce₅ quenched alloy is found to contain the Al phase, an amorphous phase and some Al₂Zn₂Ce intermetallic compounds. Whereas, the diffraction pattern of Al₈₃Zn₁₀Ce₇ alloy consists of a prepeak near 18.5°, followed by a main broad peak near 38°. The main broad peak indicates the formation of a single amorphous phase. The most interesting is the prepeak. The presence of a prepeak caused by strong interaction between unlike atoms corresponds to a cluster structure with chemical short-range order in the sense of compound formation. Al₉₀Zn₁₀ alloys have weak interaction between unlike atoms [15], so they are liable to exhibit phase separation. Upon adding Ce into Al–Zn alloys, an intermetallic compound Al₂Zn₂Ce appears, which prevents the occurrence of phase separation, and improves the forming ability of the single amorphous phase. For the Al–Zn–Ce alloy with Al content up to 80 at.% it is much easier to obtain the amorphous microstructure than for an Al₉₀Zn₁₀ alloy. Therefore, increase of Ce concentration is favorable as regards facilitation of glass formation in the Al–Zn–Ce alloys.

Quenching rate has important effects on the microstructure of rapidly solidified alloys [16]. Generally, as the quenching rate decreases, a fraction of crystal phases may

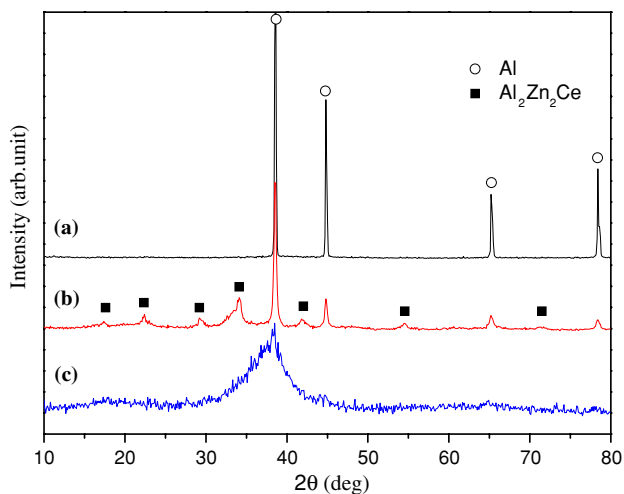


Fig. 1 X-ray diffraction patterns of (a) Al₉₀Zn₁₀, (b) Al₉₀Zn₅Ce₅, and (c) Al₈₃Zn₁₀Ce₇ alloys quenched with the circumferential velocity of 40 m/s

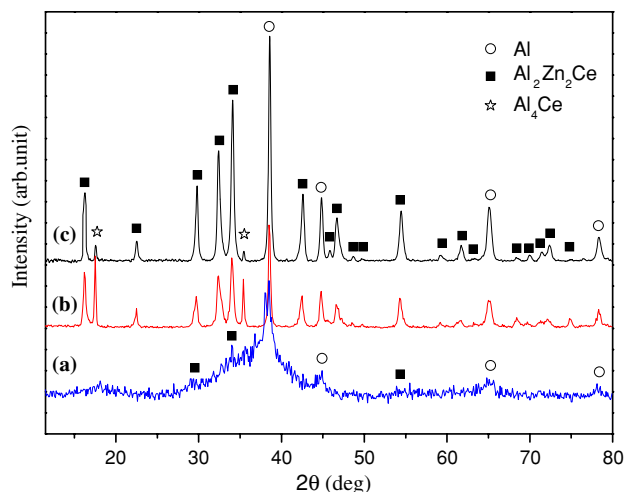


Fig. 2 X-ray diffraction patterns of Al₈₃Zn₁₀Ce₇ alloys (a) quenched with 30 m/s, (b) quenched with 20 m/s, and (c) aged at room temperature for 11 months

form from the glassy matrix. At a slow circumferential velocity, Al₈₃Zn₁₀Ce₇ quenched alloy mainly includes the fcc-Al phase, Al₂Zn₂Ce phase and a small number of Al₄Ce phase (Fig. 2b). These findings suggest that the formation of Al₂Zn₂Ce and Al₄Ce phase is prone to nucleate from the melt and they compete with the formation of the fcc-Al phase. By increasing the circumferential velocity of the copper wheel, the diffraction pattern of the Al₈₃Zn₁₀Ce₇ quenched alloy shows Al and Al₂Zn₂Ce peaks which overlap on the glassy matrix (Fig. 2a). Notably, a prepeak also can be found which is mostly related to the formation of Al₂Zn₂Ce and Al₄Ce compounds. By comparing Fig. 1b with Fig. 2b, we can infer that the nucleation and growth of fcc-Al and Al₂Zn₂Ce is easier than that of Al₄Ce. Figure 2c shows the XRD pattern of Al₈₃Zn₁₀Ce₇ alloy quenched with 20-m/s aged at room temperature for 11 months. As they were on the as-rapidly solidified Al₈₃Zn₁₀Ce₇ alloy (Fig. 2b), the same phases were found on the natural aged sample. However, the peaks of fcc-Al and Al₂Zn₂Ce become more intense and the Al₄Ce peaks become more weak which nearly disappear. It appears that the growth of fcc-Al and Al₂Zn₂Ce is preferential to that of Al₄Ce.

The DSC experiments were used to determine the crystallization process and thermal stability of the amorphous alloys. Apparently, there are two exothermic peaks in the DSC curves indicating the crystallization of Al₈₃Zn₁₀Ce₇ amorphous alloy through two stages (Fig. 3). There appears to be no resolvable endothermic peak prior to the first crystallization reaction. This implies that there may be no glass transition in the sample during the present calorimetric measurement. Tjong and Wang [17] reported the similar result by studying the DSC traces of Al₈₈Ni₉Ce₂Fe₁ amorphous alloy scanned at a rate of 0.33 K/s.

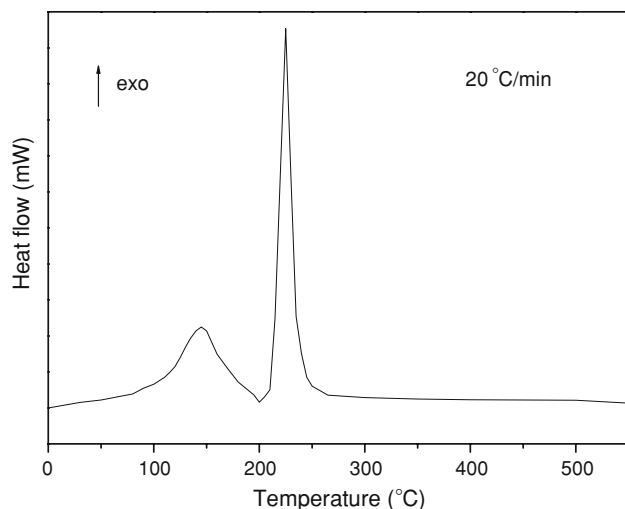


Fig. 3 DSC curve of $\text{Al}_{83}\text{Zn}_{10}\text{Ce}_7$ amorphous alloy

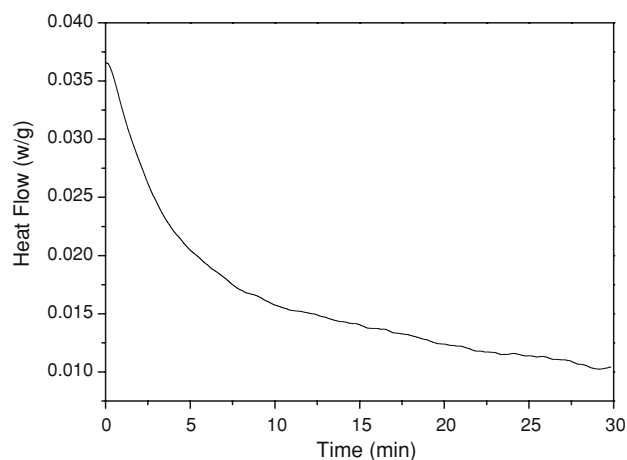


Fig. 5 Isothermal DSC trace from $\text{Al}_{83}\text{Zn}_{10}\text{Ce}_7$ amorphous alloy annealed at 105 °C for 30 min

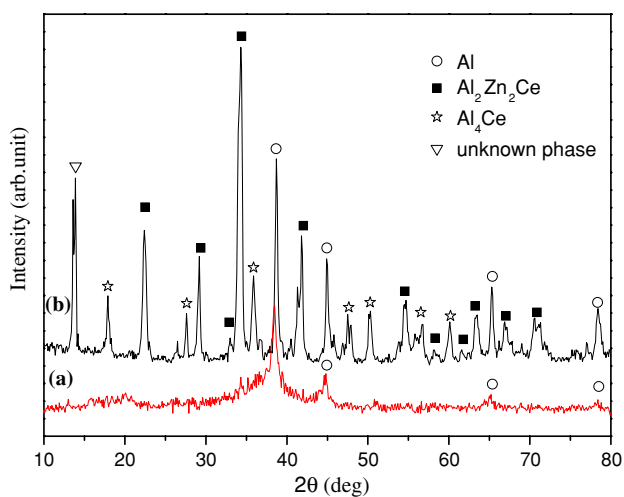


Fig. 4 X-ray diffraction patterns of the $\text{Al}_{83}\text{Zn}_{10}\text{Ce}_7$ amorphous alloy at different temperatures (a) 180 °C, (b) 275 °C

In order to trace the crystallization process, XRD patterns at different temperatures were also examined. Figure 4 shows the XRD patterns of amorphous $\text{Al}_{83}\text{Zn}_{10}\text{Ce}_7$ alloy continuously heated to 180 and 275 °C. The first temperature corresponds to the end of the first crystallization stage and the second temperature corresponds to the end of the second crystallization stage. At 180 °C, it can be seen that a fcc-Al phase appears. The prepeak exists at about 18.8°, indicating that the nature structure corresponding to the prepeak remains unchanged and more stable than the amorphous matrix. However, the prepeak has become broader, and we dare not to say that some intermetallic nuclei have not existed in the alloy. At 275 °C, several intermetallic compounds indicated as $\text{Al}_2\text{Zn}_2\text{Ce}$ and Al_4Ce phases are formed. These findings

suggest that the first exothermic peak in the non-isothermal DSC curve corresponds to the Al phase crystallization, and the second exothermic peak corresponds to the formation of the intermetallic compounds.

In order to distinguish the grain growth process from that of nucleation and growth crystallization, the isothermal DSC method has been developed [18]. During a grain growth process, the rate of evolved heat is found to monotonically decrease in an isothermal DSC scan, while the peaked signal can be observed in nucleation-and-growth process. Figure 5 shows the isothermal DSC trace at 105 °C below the onset temperature of the first exothermic reaction for $\text{Al}_{83}\text{Zn}_{10}\text{Ce}_7$ amorphous alloy. Isothermal DSC study indicates that the amorphous $\text{Al}_{83}\text{Zn}_{10}\text{Ce}_7$ alloys transform via a grain growth process. Therefore, the fcc-Al should be preexistent in the amorphous alloys.

With the aim to better understand the glass-forming ability and structural characteristic of Al-based alloys, the crystallization behavior of $\text{Al}_{83}\text{Zn}_{10}\text{Ce}_7$ amorphous alloy was studied. In the XRD pattern taken after an isothermal anneal at 145 °C for 5 min (Fig. 6a), the reflection of the $\text{Al}_2\text{Zn}_2\text{Ce}$ phase and Al_4Ce phase appears in addition to the reflection of the fcc-Al phase. The same phases were found on the sample annealed at 145 °C for 10 min with more intensity (Fig. 6b). Moreover, the presence of fcc-Al appears to favor the nucleation and growth of the $\text{Al}_2\text{Zn}_2\text{Ce}$ and Al_4Ce . It seems that the precipitation of fcc-Al was accompanied with the $\text{Al}_2\text{Zn}_2\text{Ce}$ and Al_4Ce . This could indicate that quench-in nuclei of intermetallics act as seeds for heterogeneous nucleation of Al in the glassy matrix. However, from our results, it appears that the competing $\text{Al}_2\text{Zn}_2\text{Ce}$ and Al_4Ce phases nucleate with the Al phase in $\text{Al}_{83}\text{Zn}_{10}\text{Ce}_7$ alloy. The possibility of nucleating various

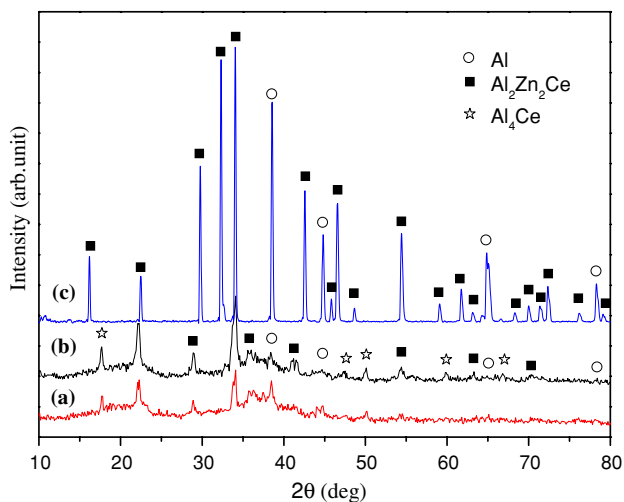


Fig. 6 X-ray diffraction patterns of the $\text{Al}_{83}\text{Zn}_{10}\text{Ce}_7$ amorphous alloy after annealing at different temperatures (a) 145 °C for 5 min, (b) 145 °C for 10 min, and (c) 550 °C

phases may represent a “confusion principle” for the alloys helping in glass formation [19]. From Fig. 6a, b, we can also confirm that the appearance of prepeak should be related to the formation of $\text{Al}_2\text{Zn}_2\text{Ce}$ and Al_4Ce intermetallic compounds. In order to examine the absolute crystallized structure of $\text{Al}_{83}\text{Zn}_{10}\text{Ce}_7$ amorphous alloy, Fig. 6c shows the XRD pattern of $\text{Al}_{83}\text{Zn}_{10}\text{Ce}_7$ amorphous alloy heated up to 550 °C far from the absolute crystallization temperature in the non-isothermal DSC curve. It is noticeable that only the diffraction peaks of fcc-Al and $\text{Al}_2\text{Zn}_2\text{Ce}$ crystalline phase emerge in Fig. 6c. This strongly suggests that the growth of fcc-Al and $\text{Al}_2\text{Zn}_2\text{Ce}$ is preferential to that of Al_4Ce and they finally eliminate Al_4Ce in the competition.

Discussion

Many metallic glasses seem to be characterized by the chemical short-range order [20]. A lot of study demonstrates that the presence of the chemical short-range order is one of the key physical factors controlling the glass-forming ability and thermal stability of the amorphous phase [21–24]. The prepeak has been observed in many Al-based alloys. The appearance of a prepeak indicates the existence of a strong chemical short-range order [9]. Moreover, the existence of the chemical short-range order in the melt of Al-based alloys has been confirmed by X-ray scattering [25], neutron scattering [26], and EXAFS [27]. It has been implied that the chemical short-range order in the Al-based metallic glasses is inherited from the melt [25]. Murdryj et al. [28] have pointed out that the chemical short-range order packed by unlike atoms could exist even

in the melt of Al–Zn with high mutual solubility. In the Al–Zn binary system, the Al-rich amorphous phase exists between α -Al phase and β -Zn phase [15]. From our results, the $\text{Al}_2\text{Zn}_2\text{Ce}$ and Al_4Ce phases are easily devitrified from the glassy matrix accompanying the precipitation of fcc-Al phase, which indicates the formation of the $\text{Al}_2\text{Zn}_2\text{Ce}$ and Al_4Ce phases is prone to nucleate from the melt. Thus, in Al–Zn–Ce alloys, adding appropriate amount of Ce changes the interaction of different atoms, leading to the formation of short-range atomic configuration mainly similar to the $\text{Al}_2\text{Zn}_2\text{Ce}$ or Al_4Ce compound, which causes Al–Zn-based alloys to form amorphous single phase by improving the compound-forming tendency and preventing the phase separation. We argue that the prepeak which indicates the existence of the strong chemical short-range order should be in favor of glass formation and structure stability of Al–Zn–Ce alloys. The previous results have suggested that the primary transformation process of Al phase is dominated by the volume-diffusion mechanism for both amorphous and nanocrystalline samples in Al-based alloys [17, 29]. With the increase of Ce concentration, this short-range atomic configuration would increase. And then the solubility of solutes would decrease as a result of the formation of this short-range atomic configuration. On the other hand, since the Ce have larger atomic radius than that of Al or Zn, adding appropriate amount of Ce would arouse large differences in atomic size between the constituent elements. The strong interaction between atoms can cause strong chemical bonding and have a certain covalent characteristic which is favorable as regards resolving difficulties of atomic diffusion and crystallization [30, 31]. The strong interaction between atoms can improve the stability of metallic glasses and favor Al-based glass formation.

High-temperature analysis indicated that a primary intermetallic starts the equilibrium solidification [13]. From Fig. 3, we could find that the precipitation of fcc-Al was accompanied with the $\text{Al}_2\text{Zn}_2\text{Ce}$ and Al_4Ce . The presence of fcc-Al appears to favor the nucleation and growth of the $\text{Al}_2\text{Zn}_2\text{Ce}$ and Al_4Ce phases. This could indicate that quenched-in nuclei of intermetallics act as seeds for heterogeneous nucleation of Al in the glassy matrix. The observation of fcc-Al plus intermetallic phases in the Al–Zn–Ce alloys suggests that the nucleation could take place during the process of rapid solidification. It is worth mentioning that the amorphous sample does not show the presence of a glass transition during the present calorimetric measurement (Fig. 3). The reason may be due to the formation of pre-existing nuclei (or small clusters). A similar case was reported by Tsai et al. [29] and they confirmed that the concentration fluctuations or pre-existing nuclei occur within the amorphous $\text{Al}_{87}\text{Ni}_{10}\text{Ce}_3$ alloy. These results also indicate that in Al-based alloys glass

formation is not controlled by nucleation restrictions. The easy nucleation is due to the existence of chemical short-range order in the melt. Therefore, to improve the suppression of growth of nuclei formed during rapid melt quenching is helpful to the high glass formation. The experimental results show that the intermetallic phases $\text{Al}_2\text{Zn}_2\text{Ce}$ and Al_4Ce competitively nucleate with the fcc-Al phase. The growth orientation of fcc-Al and $\text{Al}_2\text{Zn}_2\text{Ce}$ phases prefers to that of Al_4Ce phase. Finally, the fcc-Al and $\text{Al}_2\text{Zn}_2\text{Ce}$ phases become the main phases, and yet the Al_4Ce phase disappears in the competition. Thus, the competitive nucleation and growth limitation of the various phases are critical for the glass formation of Al–Zn–Ce alloys.

Conclusions

In summary, we have studied the amorphization and phase-selection behavior of Al–Zn–Ce alloys. The chemical short-range order in the sense of compound formation is favorable as regards facilitation of glass formation in Al–Zn–Ce alloys. It appears that the precipitation of fcc-Al was accompanied with the $\text{Al}_2\text{Zn}_2\text{Ce}$ and Al_4Ce intermetallic phases. The presence of fcc-Al phase seems helpful to the nucleation and growth of the $\text{Al}_2\text{Zn}_2\text{Ce}$ and Al_4Ce . Meanwhile, the $\text{Al}_2\text{Zn}_2\text{Ce}$ and Al_4Ce phases nucleate competitively with the fcc-Al phase in Al–Zn–Ce alloys. However, the growth orientation of Al_4Ce phase was suppressed and finally the Al_4Ce phase disappears in the competition with the growth of fcc-Al and $\text{Al}_2\text{Zn}_2\text{Ce}$ phases. The glass formation of the Al-based alloys is a strong function of the competitive nucleation and growth kinetics of various phases.

Acknowledgements This study was supported by the Natural Science Foundation of Shandong Province (Project No. Y2006B25).

References

- Scudino S, Surreddi KB, Sager S, Sakaliyska M, Kim JS, Loser W, Eckert J (2008) *J Mater Sci* 43:4518. doi:10.1007/s10853-008-2647-5
- Inoue A, Ohtera K, Tsai AP, Masumoto T (1988) *Jpn J Appl Phys* 27:L280
- He Y, Poon SJ, Shiflet GJ (1988) *Science* 241:1640
- Kim YH, Inoue A, Masumoto T (1990) *Mater Trans JIM* 31:747
- Gloriant T, Greer AL (1998) *Nanostruct Mater* 10:389
- Audebert F, Vasquez S, Gutierrez A, Vergara I, Alvarez G, Escorial AG, Sirkin H (1998) *Mater Sci Forum* 269–272:837
- Guo FQ, Poon SJ, Shiflet GJ (2000) *Mater Sci Forum* 331–337:31
- Egami T (1996) *J Non-Cryst Solids* 205–207:575
- Elliot SR (1991) *Phys Rev Lett* 67:711
- Zhang PN, Li JF, Hu Y, Zhou YH (2008) *J Mater Sci* 43:7179. doi:10.1007/s10853-008-3019-x
- Qin JY, Bian XF, Sliusarenko SI, Wang WM (1998) *J Phys Condens Matter* 10:1211
- Xu Y, Wang YL, Liu XJ, Chen GL, Zhang Y (2009) *J Mater Sci* 44:3861. doi:10.1007/s10853-009-3523-7
- Ronto V, Battezzati L, Yavari AR, Tonegaru M, Lupu N, Heunen G (2004) *Scr Mater* 50:839
- Wang SH, Bian XF (2007) *J Alloys Compd* 44:135
- Zhang L, Wu Y, Bian X, Xing Z (1999) *J Mater Sci Lett* 18:1969
- Zhang YH, Liu YC, Han YJ, Wei C, Gao ZM (2009) *J Alloys Compd* 473:442
- Tjong SC, Wang JQ (2001) *Z Metallkd* 92:610
- Chen LC, Spaepen F (1988) *Nature* 336:366
- Rizzi R, Baricco M, Borace S, Battezzati L (2001) *Mater Sci Eng A* 304–306:574
- Sheng HW, Luo WK, Alamgir FM, Bai JM, Ma E (2006) *Nature* 439:419
- Chen GL, Hui XD, Fan SW, Kou HC, Yao KF (2002) *Intermetallics* 10:1221
- Tanaka H (2005) *J Non-Cryst Solids* 351:678
- Bian X, Hu L, Wang C (2006) *J Non-Cryst Solids* 352:4149
- Mechler S, Schumacher G, Zizak I, Macht MP, Wanderka N (2007) *Appl Phys Lett* 91:021907
- Zhang L, Wu Y, Bian X, Li H, Wang W, Li J, Lun N (1999) *J Phys Condens Matter* 11:7959
- Maret M, Pomme T, Pastarel A, Chieux P (1990) *Phys Rev B* 42:1598
- Jacobs G, Egry I, Holland-Moritz D, Platzek D (1998) *J Non-Cryst Solids* 232–234:396
- Murdryj SJ, Galchak VP, Baskin VN, Skutor AK (1993) *Raspilav* 3:11
- Tsai AP, Kaniyama T, Kawamura Y, Inoue A, Masumoto T (1997) *Acta Mater* 45:1477
- Sharma SK, Strunskus T, Ladebusch H, Zaporozhchenko V, Faupel F (2008) *J Mater Sci* 43:5495. doi:10.1007/s10853-008-2834-4
- Nguyen HV, Kim JS, Kwon YS, Kim JC (2009) *J Mater Sci* 44:2700. doi:10.1007/s10853-009-3354-6